Advances in Science and Technology Research Journal

Advances in Science and Technology Research Journal, 2025, 19(5), 307–320
https://doi.org/10.12913/22998624/201428
ISSN 2299-8624, License CC-BY 4.0

Received: 2025.02.09
Accepted: 2025.03.15
Published: 2025.04.01

Small buffers manufactured by fused deposition modelling and thermoplastic elastomer filament

Jacek Wojnowski[1*]

[1] Maritime University of Szczecin, Wały Chrobrego 1/2, 70-500 Szczecin, Poland
* Corresponding author's e-mail: j.wojnowski@pm.szczecin.pl

ABSTRACT

Additive manufacturing (AM) technologies are an excellent tool for shaping the properties and producing prototypes of innovative parts and devices. The scarcity of research on bumpers made from thermoplastic elastomers (TPE) prompted efforts to expand the available knowledge. The aim of the study was to determine the influence of the hardness of the filament material, the number of walls and the fill density on the determined characteristics, i.e. maximum forces, plastic deformation, absorbed energy (EA), hysteresis and specific damping capacity (SDC) of cylindrical-shaped bumpers with a volume of 1 cm^3. The bumpers were subjected to uniaxial compression tests to deformations ranging from 0 to 70%. The above parameters of the buffers were determined by numerical integration of the relevant sections of the compression force vs displacement characteristics. The results show a non-linear dependence of the analysed parameters as a function of strain. It turned out that the type of the material had the greatest effect on the determined characteristics, followed by the filling density and the number of buffer walls was the smallest. The highest levels of technical performance were exhibited by a bumper made from a higher hardness filament, with a wall count of 8 and 100% infill density. The bumper made of the thermoplastic elastomer UNIFLEX 120, with a wall number of 8 and a filling density of 100%, showed the highest values of characteristics; the maximum force was 6.640 kN, the EA was 3.58 J, the maximum hysteresis was 1.82 J, with a plastic deformation of 38.6% for 60% deformation. The other types of bumpers, which differed in the type of filament material, number of walls and filling density, showed lower values of mechanical characteristics.

Keywords: additive manufacturing, energy dissipation, mechanical characteristics, buffers, thermoplastic elastomers.

INTRODUCTION

Bumpers

Elements that protect against the effects of unintentional collisions of objects, regardless of their size, are called buffers. The purpose of using a buffer is to reduce the momentum energy and amplitude of the forces acting on the system in question. For the protection of technical structures, rubber buffers of considerable size are usually used [1, 2]. Medium-sized buffers can be part of damping systems made up of, among other things, a hydraulic shock absorber, elastomeric inserts and a steel casing, e.g. the Keystone train bumper with Combigard T 105 (train bumper) [3]. Classical elastomeric small-size buffers can be used to protect walls against the impact of doors, gates. The use of small-size buffers made of new materials should not be ruled out to replace rubber buffers in their existing solutions.

Additive manufacturing technologies

Additive manufacturing technologies, often referred to as 3D printing, are seeing continued growth and revenue growth from $18.0 billion in 2022 to a projected $102.7 billion in 2032 [4]. There is no indication that the trends in AM will change in the coming years. An analysis of the number of patents granted and revenues related to incremental technologies in the work [4] also confirms this observation.

AM technologies, in relation to low-volume injection moulding production, are characterised

by lower product manufacturing costs and shorter lead times [5]. AM technologies can be successfully used to produce small bumpers due to the following characteristics:

- Fast designing and prototyping – short time from design to final product [5, 6]. On the basis of the acquired knowledge of the mechanical energy damping of buffers, products with application-specific characteristics can be designed in a very short time. They can be "tested" and implemented by the customer, allowing adjustments to be made to the product at the initial stage of the buffer use.
- Variety in designs – to meet the requirements of a given customer group and meet the demand for prints with precise geometries [6, 7]. Buffers with precise geometries can be easily designed in widely available CAD software.
- Enhanced product range – By using AM technology, a given company can provide a wide range of prints for each customer. The range can thus be diversified [6]. There can be a significant number of buffers on offer due to the ease of modifying the geometry and internal structure of the print [7].
- Improved quality – small production cycles provide the opportunity to improve products at the design stage and actual production [6]. Buffers with new mechanical characteristics can be investigated at this stage.
- Smoother production process – product development does not interrupt or interfere significantly with the production process [6]. In order to carry out the research on buffers, the production process does not need to be interrupted, because it can be carried out on a small number of printers. Production can be successfully carried out continuously.
- Comparative advantage – low lead times, no precision moulds required as in injection moulding, less material used in production [5, 6]. The bumpers produced using AM technology and low-volume production mode are obtained faster and more efficiently, with lower material consumption.
- Cost advantage – enables the design and production of small quantities of prototypes and tools in-house (rapid tooling) and allows the R&D costs to be significantly reduced [5, 6].
- Minimal material waste – prints can be produced with a minimum of post-production waste [6]. The buffers as well as the model supports produced using the fused deposition modelling (FDM) method are made of thermoplastic and can be recycled and reprocessed.
- Mass customisation – AM technologies, sometimes combined with injection moulding, have the ability to produce prints with different geometries and properties, which is not possible with injection moulding technologies alone [8].

The manufacture of products using AM technologies is based on the construction of the product layer by layer, based on a 3D model in digital form and a given physical phenomenon. The operating principles of the various additive technologies are described in detail in work [9] and will not be described further here.

There are seven incremental manufacturing technologies [10]: binder jetting (BJ), direct energy deposition (DED), material extrusion (alias FDM), material jetting (MJ), powder bed fusion (PBF), sheet lamination (SL), and VAT polymerisation.

Of the above-mentioned technologies, four can be applied to the processing of polymeric materials that ultimately have elastomeric characteristics, i.e. low hardness, very high strain to failure, low Young's modulus, low proportion of permanent deformation. These are BJ, FDM, PBF and VAT Polymerisation [11].

Strengths of the FDM technology

Indirectly, the price of equipment and material in a given technology is a determinant of its usefulness for producing specific products and selling them on the market. The price of the printers and the thermoplastic elastomer filament used for printing is still in favour of the FDM technology. The cost of BJ printers is up to 200 000 PLN with material cost starting from 1 600 PLN. The cost of FDM printers ranges from PLN 1 to PLN 10 000. Filament costs between PLN 100 and 300 per kg. Printers in PBF and VAT Polymerisation technology cost up to PLN 75 000 and PLN 200 000, respectively. The cost of powder for printers in PBF technology is PLN 680/kg, while the cost of resin, which after cross-linking has elastomer characteristics, is PLN 320/kg. The cost/effect ratio is in favour of the FDM technology. FDM printers are already present in every institution; from schools and universities to small and large businesses [12]. Undoubtedly, the price of the printers and the thermoplastic elastomer filament used for printing is still in favour of the FDM technology.

FDM does not require significant skills (expertise) from the technologist/printer like PBF and VAT Polymerisation technology [12]. The accuracy of model reproduction in FDM technology is worse in relation to PBF and VAT Polymerisation, but still sufficient for technical applications [12].

Literature sources indicate that prints in the FDM technology can be subjected to: machining [13], chemical treatment to improve surface quality [14], or thermal treatment, which affects the final properties of the print, including mechanical properties and surface quality [15]. Multi-material printing allows complex prints with new and unprecedented properties to be obtained in a single step [16]. The FDM technology is also characterised by: short and undemanding post-processing (removal of supports and the base of the print), material recycling of waste after the printing process, or the production of products with closed surfaces and different infill densities, without the need to remove the remaining material from the closed interior voids of the print, which affects the weight and final properties of the print [17].

On the basis of the information cited above, it can be concluded that the FDM technology is an excellent solution for printing a variety of small-sized components. Such products include the buffers presented in this publication.

Thermoplastic elastomer and rubber as damping materials

The display of a significant level of mechanical damping by rubbers [18, 19] as well as thermoplastic elastomers [20, 21] is a well-known phenomenon. During the deformation of vulcanised rubber [2, 22], as well as thermoplastic [23] elastomer products, a characteristic hysteresis loop appears, which is the result of the elastomer dissipating strain energy.

Table 1 provides concise information on which characteristics of a buffer made of rubber and thermoplastic elastomer can affect its ability to dissipate mechanical energy. The microstructure of the material and the macrostructure of the buffer affect the ability to absorb mechanical energy. Thermoplastic elastomers, compared to rubber, due to the physical nature of the network nodes, have a poorer resistance to prolonged static forces, so-called creep, and a high level of plastic deformation [24] (p. 224–225). On the other hand, physical network nodes allow processing using the FDM technology and shaping the physical properties of buffers over a wide range. Thus, it becomes reasonable to analyse the possibility of using TPE in the construction of innovative buffers produced using the FDM technology.

Thermoplastic urethane elastomer (TPE-U) filament has been used to produce, among other things, strain [33] and force sensors [34], parts with shape memory [35] and that deform under electrical potential [36], magnetic properties [37] and mechanical properties [38, 39]. TPE-U has also been studied for medical applications [40, 41]. TPE-U was used in the study of composite structures [42, 43]. The group of thermoplastic elastomers also includes ethylene-vinyl acetate (EVA) copolymers. Although they have been studied, they have not yet gained popularity among users of FDM 3D printers [44, 45]. A less common material for use in FDM 3D printing is styrenic thermoplastic elastomer (TPE-S). This type of TPE has a wide range of hardness and mechanical properties, good damping and does not require drying before processing and is easy to print. These characteristics determined the use of TPE-S to produce the bumpers described in this study. There are reports in the literature of the use of TPE-S for printing capacitive force sensors, mechanical vibration dampers [46] and pressure sensors [47].

Wojnowski and Chmiel [48] investigated the ability of soft material thermoplastic elastomer prints (UNIFLEX 75 from 3D UNIVERSAL) to dampen mechanical vibrations in the X-Y plane of shear forces. Depending on the geometry of the print and the degree of filling, the damper showed

Table 1. Factors influencing the dissipated energy of a buffer made of rubber and thermoplastic elastomers

Factor	Rubber	Thermoplastic elastomer
Chemical structure	Major impact [25]	Major impact [26, 27]
Prestrain	Small impact [28]	Major impact [29]
Ability to achieve a complex external buffer geometry	Capability low and limited by the geometry of the mould [30]	Significant [31, 32]
Ability to achieve a complex internal buffer geometry	No internal, 3D printing like, geometry possible [30]	Significant [7]

a different vibration damping capacity. The degree of filling of the print – the cylinder – mattered and the maximum damping appeared for a infill density value of 50%, while for 0% and 100% the values of dissipated energy turned out to be lower.

León-Calero and coauthors [7] conducted an analysis of quantities such as compression strength, specific energy absorption, compression modulus, SDC for samples differing in internal structure, fill density and type and hardness of the filament material. These proved to have a significant effect on the determined quantities. For increased material hardness of one type and infill density, compression strength increased. the best results for the quantities related to mechanical energy dissipation were obtained for the material with the highest hardness and the highest fill density.

Printing parameters

Printers operating in the FDM technology have a significant number of technological parameters (e.g. infill angle, infill density, infill type, layer thickness, nozzle temperature, printing bed temperature, head movement speed, air gap) that affect the final print mechanical properties [49]. On the basis of the author's previous experience with thermoplastic elastomer filaments, it was found that the type of filament material, number of walls and infill density can have a significant impact on mechanical properties, including the dissipation of impact energy.

Quantities describing the buffer's ability to dissipate mechanical energy

León-Calero et al. describes in detail the behaviour of prints obtained by the FDM technology subjected to compression [7]. The quantities determined are: hysteresis, energy absorption, specific damping capacity. Xu et al. additionally introduces the parameter specific energy absorption [50]. In the light of studies on the energy dissipated by buffers with inhomogeneous internal structure, i.e. different material distribution on the cross-section, specific energy absorption is a difficult quantity to estimate. The author of this publication decided to use hysteresis, EA and SDC to describe the deformation behaviour of small-sized buffers in a uniaxial pseudocyclic compression test as adequate energy parameters.

Novelty

An element of novelty in this publication is the use of the FDM 3D printing technology to produce buffers. The FDM technology allows for the shaping of mechanical properties [51, 52], damping [7, 53] and geometry of prints [48, 52]. Thus, it becomes reasonable to see, by experiment, what possibilities FDM offers in shaping the mechanical properties and damping of mechanical energy of small buffers made from a flexible filament of the TPE-S group. An element of novelty is also the initial proposal to use "stacks" of individual buffers in the bumper (Fig. 1).

Figure 1 shows an example of the use of buffers analysed in this study. Small-sized buffers can be used as an impact energy absorbing element. They can be stacked with buffers of a single type as well as with buffers of different types. The second solution would allow the mechanical characteristics of the entire impact energy absorbing system to be mixed. This is a prototype device that is worth testing under real conditions.

Objective and summary

The results of a database search (www.webofscience.com) on the following keywords:

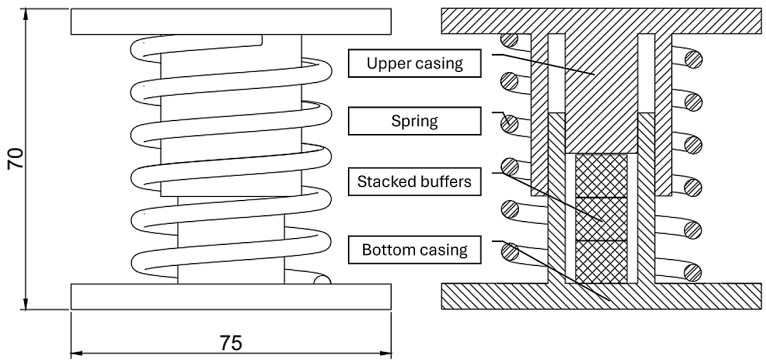

Figure 1. Example of the use of small-sized buffers in a vehicle bumper

FDM, FFF, buffer, bumper, damper, thermoplastic elastomer, either yielded no results or the publications were completely unrelated to the topic addressed in this publication.

The aim of this publication is to analyse the extent to which the model wall count and infill density influence permanent set and hysteresis, EA and SDC as quantities related to the mechanical energy dissipation of a buffer of a given type.

MATERIALS AND METHODS

Printer setup and CAD model

The buffers under study were manufactured on a MakerBot Replicator 2X printer (manufacturer based in the United States), operating in FDM extrusion technology. On the basis of the information obtained from the literature [7], the author decided to use a buffer with a cylindrical shape (Fig. 2).

The dimensions of the buffer – a height of 10 mm and a diameter of 12 mm – were determined by first arbitrarily assuming a buffer height of 10 mm and then, based on EN ISO 604:2003 (Equation 1), calculating the diameter for which the buffer would not buckle and rounding up to a whole number:

$$\varepsilon_c^* \leq 0.4 \cdot \frac{x^2}{l^2} \tag{1}$$

where: ε_c* – maximum nominal compression strain; l – buffer length, x – buffer diameter.

The model in digital form was prepared using FreeCAD software. Commercial UNIFLEX 75 and UNIFLEX 120 filaments (TPE-S class polymer) from 3D UNIVERSAL, Poland, with a diameter of 1.75 mm and two hardnesses (75 and 120 Shore A, values given by the manufacturer) were used.

The technological parameters of the 3D printer, which were not changed during the manufacturing process of the buffers, were as follows: type of infill – linear, printing temperature = 245 °C (UNIFLEX 75) and 225 °C (UNIFLEX 120), height of the printed layer = 0.20 mm, cooling of the print by air flow - maximum available. The technological parameters that were changed are given in Table 2.

Uniaxial pseudocyclic compression test

The buffers were subjected to a uniaxial pseudocyclic compression test using an Autograph AG-X plus (Shimadzu, Kyoto, Japan) tensile testing machine. Deformation was carried out until the crosshead reached a displacement of 1, 2, 3, 4, 5, 6, 7 mm from the initial position of 0 mm. The crosshead of the testing machine was returned to the position where the force value was 0 N. A sensor with a force measurement range of up to 10 kN was used for the tests. The speed of movement of the crosshead was constant and equal to 5 mm/min. Where required, the corresponding crosshead displacement values of the testing machine were converted to values of buffer deformation and expressed in %.

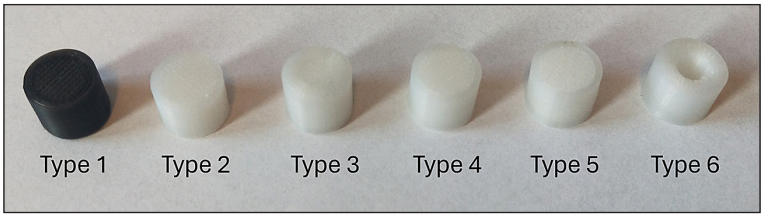

Figure 2. Geometry of buffers analysed in this study

Table 2. Type and technological parameters changed during manufacturing process of buffers

Designation	Filament	Infill density	Model wall count	Number of samples tested
Type 1	UNIFLEX 75	100%	3	3
Type 2	UNIFLEX 120	100%	3	3
Type 3	UNIFLEX 120	100%	8	3
Type 4	UNIFLEX 120	70%	3	3
Type 5	UNIFLEX 120	50%	3	3
Type 6	UNIFLEX 120	0%	8	3

The designations and the first hysteresis loop, an example for each type of buffer, are shown in Figure 3. Abbreviations and designations used will be explained below.

The level of permanent set for a given strain value was determined using the graphs shown in Figure 4. The x_{ui} value for the i-th cycle was read and then strain was determined by dividing it by the bumper height of 10 mm. The result was the dependence of permanent set as a function of maximum strain for a given cycle.

From the graphs (Fig. 4), the values of hysteresis (A) for a given strain were determined [7] Equation 2:

$$Hysteresis = A = \\ = \int_{x_{ui}}^{x_{li}} F_{L,II}(x)dx - \int_{x_{li}}^{x_{ui}} F_U(x)dx, \text{ for i} = 1,..,6 \quad (2)$$

where: x_{li} – displacement after loading, x_{ui} – displacement after unloading, i – deformation cycle number, $F_{L,II}$ – curve for second loading cycle, F_U – curve for unloading step.

The hysteresis is the difference between the work applied to the buffer during loading and the work recovered during unloading, and directly represents the amount of energy that is lost irretrievably in the way of heat to the environment [54].

Knowing the course of the F-x curves (Fig. 4), it was possible to determine the energy absorption using Equation 3 below [7].

$$EA = A + B = \\ = \int_{x_{ui}}^{x_{li}} F_{L,II}(x)dx, \text{ for i} = 1,..,6 \quad (3)$$

Equation 3 designations are the same as in Equation 2. The EA value represents the work involved in deforming the buffer, without taking into account the energy returned to the environment (B). When comparing two buffers, the first with a lower and the second with a higher EA value, the latter will require more energy to deform the buffer by a given amount, such as 10%.

EA and hysteresis were calculated using numerical integration, using the trapezoid method, as indicated in the diagram below (Fig. 3). The unit of EA and hysteresis was the unit of energy – Joule.

Integration was carried out on a selected representative curve, for each type of buffer. The selection of the representative curve was done subjectively, assuming that the representative curve lay between the curve with the largest values and the smallest values.

Specific damping capacity is the ratio of A to the sum of A and B [7] Equation 4:

$$SDC = \frac{A}{A+B} \cdot 100\% = \\ = \frac{Hysteresis}{EA} \cdot 100\% \quad (4)$$

The higher the SDC of the buffer, the greater the proportion of hysteresis in the total work involved in its deformation. For hypothetical cases, an SDC of 100% indicates that virtually all the work involved in deforming the bumper is dissipated in the way of heat. For SDC values close to 0%, the bumper shows no damping, while all the strain energy is returned back to the system. Ideally, buffers should exhibit high SDC values. The unit of SDC is %.

Statistical analysis

Tests on the testing machine were carried out on 3 buffers of each type (Table 2). A separate

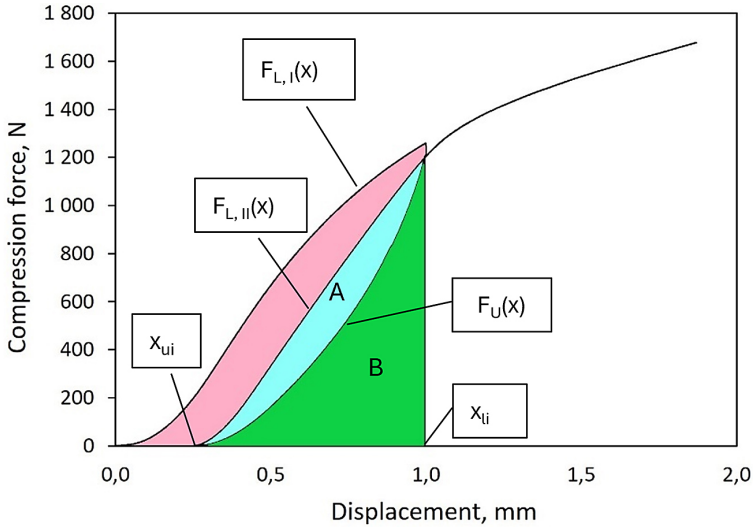

Figure 3. Compression force vs testing machine crosshead displacement

analysis was carried out for each buffer by calculating: permanent set, hysteresis, EA, SDC.

The curves in the graph (Fig. 4) are single and representative of each type of buffer. They were selected as the curves lying between the extremes – with the highest and lowest values.

The values on both the X and Y axes of Figures 5–8 were the arithmetic mean of the values from each of the three samples.

The values in the table (Table 3) are the maximum values obtained for a given buffer type.

RESULTS

General mechanical characteristics of buffers

Thermoplastic elastomers with a high percentage of soft phase and during deformation, TPE-U [55], TPE-E [56], TPE-V [28], exhibit the Mullins effect [57], hysteresis and a certain level of reversible and irreversible deformation. The curves produced by pseudocyclic deformation of buffers (Fig. 4) are of a nature inherent to the deformation of TPE products. Pseudocyclic deformation, in contrast to cyclic deformation, is led to increasing strain values [23]. Repeating the load-unload cycle for a given maximum strain value is not required, as it does not significantly affect the mechanical characteristics [28].

The deformation of TPE is accompanied by the Mullins effect of destroying the original microstructure. What results is a lower force level of the second loading cycle of the material $F_{L, II}(x)$ compared to the first $F_{L, I}(x)$ (Fig. 3). If the material is not subjected to higher deformations than the current and maximum deformations in a given cycle, it will continue to operate based on the existing hysteresis loop of $F_{L, II}(x)$ and $F_{U}(x)$. As the number of deformation cycles increases, there is a slight/negligible reduction in the stress level of the hysteresis loop [28]. Thus, it was considered unnecessary to run the deformation more than twice for one cycle – once to show the Mullins effect and a second time to determine the hysteresis loop. The curves (Fig. 4) do not have a clear plateau and do not show plastic flow during deformation of the buffer.

The type of filament material from which Type 1 and Type 3 buffer is constructed has a significant impact on the mechanical characteristics. The use of a material with a lower Shore A hardness for printing bumpers results in lower levels of permissible forces that the buffer can transmit without risk of failure. Different characteristics are obtained for the UNIFLEX 120 material (Fig. 4), which is undoubtedly related to the buffer's macrostructure, the number of model walls and the infill density. The UNIFLEX 75 soft-filament buffer is not able to carry loads greater than 0.635 kN (for a crosshead displacement of 6 mm), so as not to be destroyed.

Type 2 and 3 buffers were found to have identical mechanical characteristics. Hence, it was concluded that the number of walls is not important in the process of determining the technological parameters of the print and can be assumed to be 3 or 8, depending on the application. Under the given test conditions, buffers of type 2 and 3 transfer the highest compressive forces, equal to 6.415 kN and 6.640 kN, respectively, for a crosshead displacement of 7 mm.

Analysis of the mechanical characteristics shown in Figure 4, which apply to buffers of types 2, 4 and 5, leads to the conclusion that the density of filling of the buffer has a significant effect on the level of compression forces. The infill density

Table 3. Potential applications for buffers

Designation	Maximum load	Maximum permanent set	Maximum hysteresis	Applications
Type 1	<0.635 kN	<11.0%[1]	<0.32 J[1]	Dampers under lightweight equipment or buffers for doors and gates
Type 2	<6.415 kN	<37.7%	<1.81 J	Stacking buffers to protect motor vehicles or dampers for heavy equipment
Type 3	<6.640 kN	<38.6%	<1.82 J	Stacking buffers to protect motor vehicles or dampers for heavy equipment
Type 4	<4.405 kN	<33.9%	<1.10 J	Stacking buffers to protect motor vehicles or dampers under medium weight equipment
Type 5	<2.880 kN	<31.3%	<0.66 J	Stacking buffers to protect motor vehicles or dampers under medium weight equipment
Type 6	<3.635 kN	<35.7%	<0.97 J	Stacking buffers to protect motor vehicles or dampers under medium weight equipment

Note: [1] approximated value.

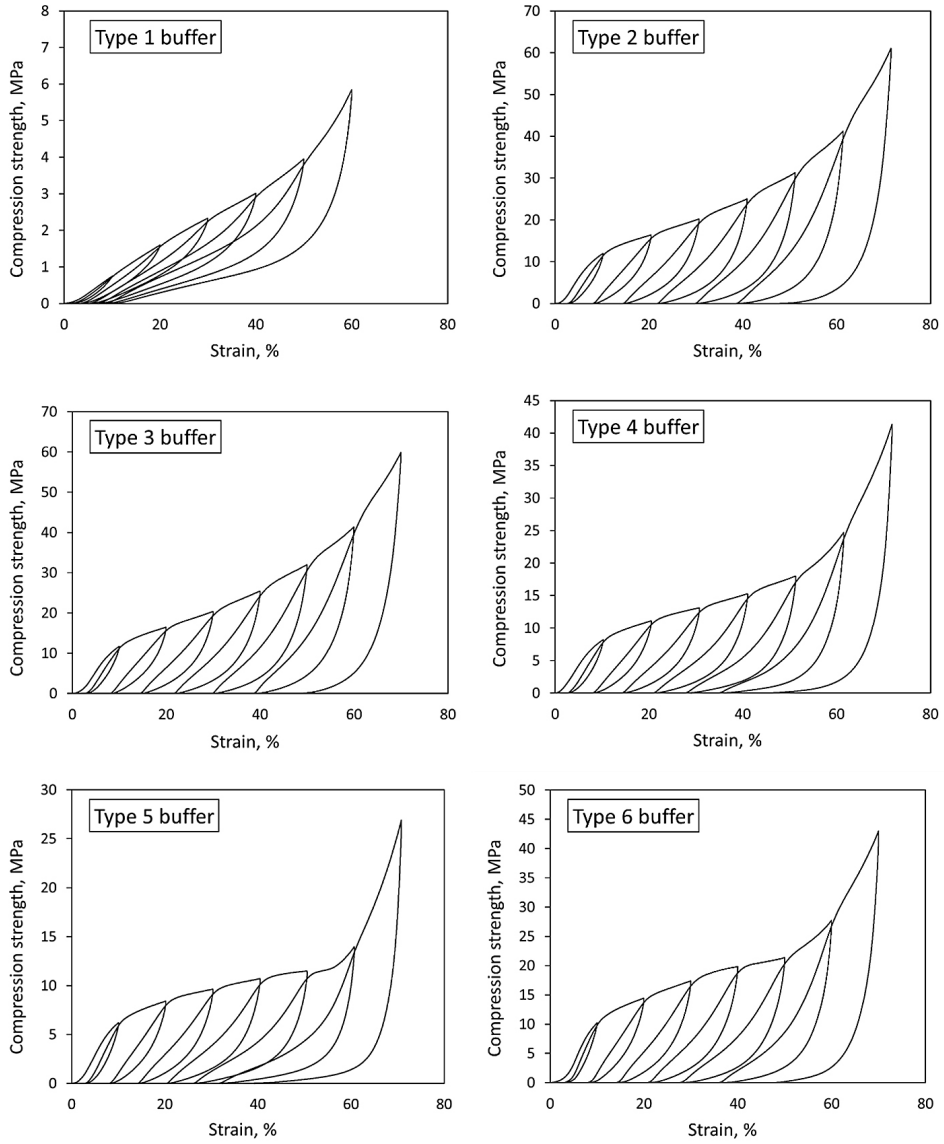

Figure 4. Compressive force – machine crosshead displacement characteristics for each type of buffer

influences the slope coefficient of the data at the start (0 to 1 mm displacement), middle (1 to 6 mm displacement) and end (6 to 7 mm) of the mechanical characteristics above.

Permanent set

On the basis of the characteristics presented above (Fig. 4), a graph of the dependence of the plastic strain contribution as a function of the maximum deformation during the cycle was drawn up (Fig. 5). During the deformation of the buffers, above the maximum deformation reached in the previous cycles, there is an increase in the proportion of irreversible deformation [23]. The type 1 buffer exhibits the lowest proportion of permanent set over the entire range of deformations tested. The buffers manufactured from a lower hardness filament are characterised by a lower level of irreversible deformation.

The plastic deformation contribution curve for the buffers of types 2 to 6, for a deformation equal to 30%, has an identical course. In the deformation range from 0 to 30%, the effect of wall number and infill density on plastic deformation is negligible.

Above a deformation value of 30%, the level of plastic deformation varies. Type 3 buffer achieves the highest level of plastic deformation of 38.6% (Fig. 5), while type 5 buffer achieves the lowest, up to a maximum of 31.3%, for a deformation of 60%. This represents a 19% decrease in the level of plastic deformation exhibited by the type 5 buffer compared to type 3. The lower wall

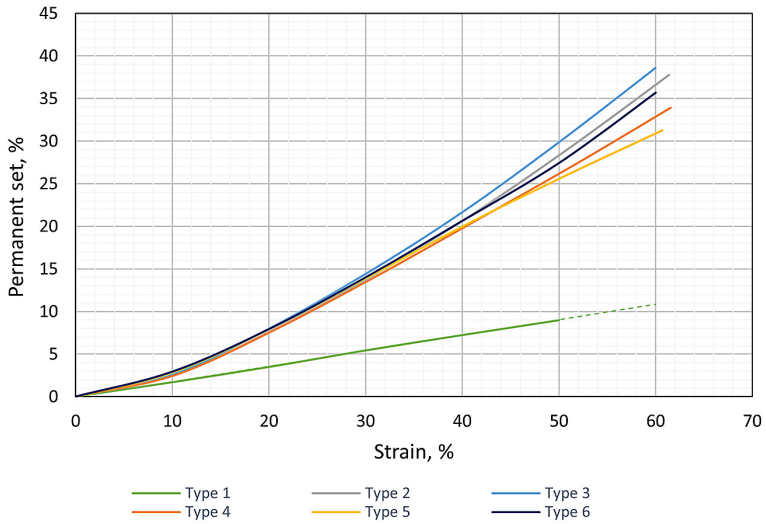

Figure 5. Contribution of permanent set as a function of buffer strain. Dotted line – extrapolated Type 1 permanent set

number affects the level of plastic deformation of the buffers. For type 2 buffer with a wall number of 3, the plastic deformation characteristics have lower values than type 3 buffer with a wall number of 8. The infill density affects the level of plastic deformation, reducing its contribution to the total deformation over the cycle, with a decrease in the infill density of the buffer.

Energy absorption

Using the knowledge of the 'force-displacement crosshead' curves (Fig. 4), it is possible to analyse the energy absorbed by the buffer during deformation. The graph (Fig. 6) shows the EA curves for the buffers as a function of maximum deformation per cycle. The type of material has a significant effect on the work consumed to deform the buffer. For a deformation of 50%, the EA of type 2 buffer is at least four times that of a type 1 buffer. Hence, to increase the overall work to deform the buffer, it is sufficient to use a material with a higher hardness. The number of buffer walls affects the EA level. It decreases as the number of walls decreases; as can be seen for type 2 and 3 buffers. As the infill density decreases from 100% through 70% to 50% – type 2, 4 and 5 buffers – show decreasing EA values throughout the deformation range. Infill density plays a key role in the buffer's EA level. To increase the overall EA level, higher values of print infill density should be used.

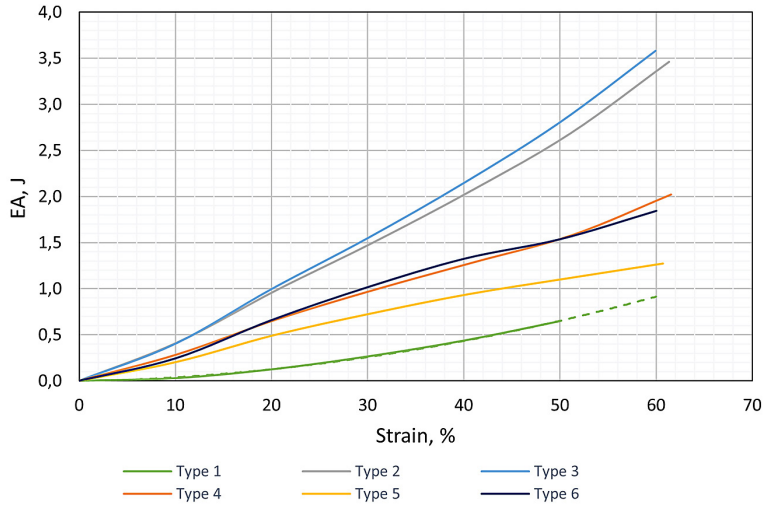

Figure 6. Contribution of energy absorption as a function of buffer strain. Dotted line – extrapolated Type 1 EA

Hysteresis

For each value of maximum deformation in the cycle, the corresponding hysteresis value was determined and plotted in the graph below (Fig. 7). The hysteresis curves as a function of buffer strain have a characteristic non-linear pattern and are increasing. Up to a deformation of 5%, the hysteresis curve increases slightly. It is only in the deformation range from 5% to 60% that it increases abruptly. For small deformations and for buffer types 2 to 6, the effect of wall number and infill density on the hysteresis is negligibly small.

The buffers made of higher hardness filament material exhibit the highest levels of hysteresis. For a deformation of 60% and compared to type 1 buffer, type 2 buffer has almost six times the hysteresis. The number of walls of type 2 and type 3 buffer, for an infill density of 100%, slightly affects the level of hysteresis exhibited. Type 3 buffer with a wall number of 8 shows higher hysteresis values. The infill density has a significant effect on the hysteresis of the buffers.

Specific damping capacity

Knowing the hysteresis and EA characteristics, it was possible to determine SDC as a function of buffer strain (Fig. 8). The SDC value for a given buffer structure is strain-dependent and increases along with strain. The influence of the material on SDC (buffer types 1 and 2) is evident in the deformation range of 10–20%. For the UNIFLEX 75 material and the aforementioned range of deformations, SDC takes on lower values, which means that the material with the lower hardness shows worse damping of mechanical vibrations. An unambiguous determination of the effect of wall number and infill density on SDC, for buffers of types 2 to 6, is subject to considerable error due to the overlap of the curves in the 20–60% strain range.

Buffers analysed and potential applications

On the basis of the results presented, several examples of buffer applications can be given (Table 3). If the buffer meets the need to transmit very high forces and a significant ability to dampen impacts, type 2 or 3 buffer should be used. For undemanding applications, type 1 buffers can be used, which are characterised by a minimum degree of irreversible deformation and low transmitted forces.

DISCUSSION

General

In the source [7], the authors present results showing a significant effect of hardness on EA, where for a filament hardness of 95 ShA there is a significant increase. In the present study, a similar phenomenon was observed for type 1 and type 2 buffers, produced from TPE with hardness of 75 ShA and 120 ShA. Such a phenomenon may be due to the lower proportion of flexible segments [23] in the UNIFLEX 120 filament, which consequently leads to higher deformation resistance at the molecular level and an increase in EA values.

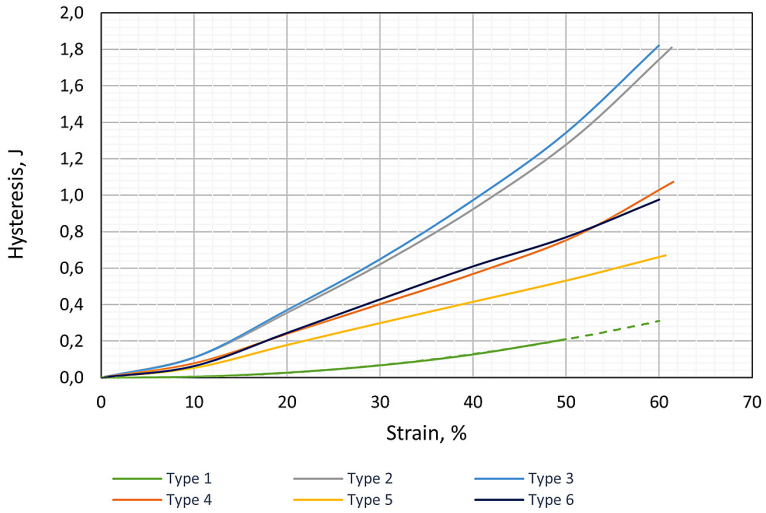

Figure 7. Contribution of hysteresis as a function of buffer strain. Dotted line – extrapolated Type 1

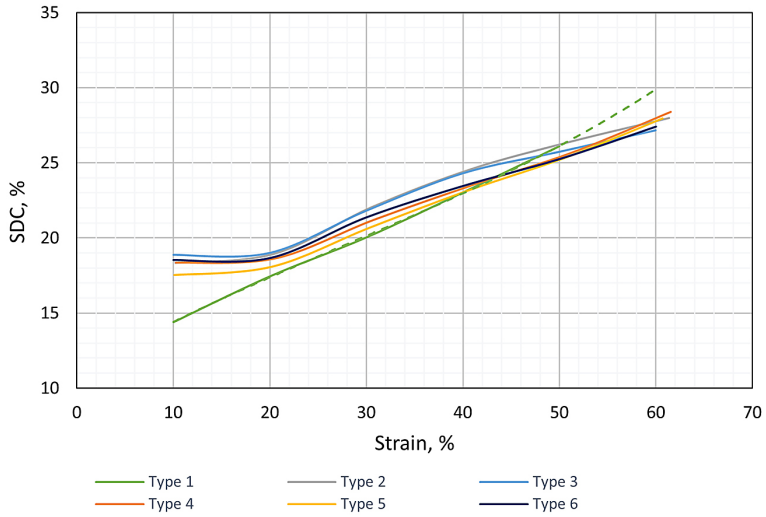

Figure 8. Contribution of SDC as a function of buffer strain. Dotted line – extrapolated Type 1.

As expected, it was found that the hysteresis value increases along with infill density of the buffer. This is confirmed in [7], where León-Calero et al. present the results of analyses of the dependence of SDC as a function of infill density of TPE samples. However, the effect of infill density in the cited publication is ambiguous.

The test results, as expected, confirmed the conjecture that infill density should significantly affect EA, hysteresis, and SDC. Moreover, as infill density decreases, the mentioned characteristics should also decrease. It was confirmed that the plastic strain values of the buffers increase along with the cycle strain. The differences in the EA, hysteresis and SDC of buffers type 1 and 2 can be explained by the higher proportion of the soft phase in the UNIFLEX 75 material. The plastic deformation, EA, hysteresis and SDC of TPE buffers can be shaped over a wide range, most effectively by selecting, first, the TPE used, then the print infill density and finally the number of print walls.

Disadvantages of presented solution and way to solve them

In addition to the obvious advantages of FDM-produced buffers, this solution has some disadvantages that need to be mentioned here.

The deformation of TPE products to increasing levels is always accompanied by the phenomenon of increasing plastic deformation [23]. Furthermore, as shown in this publication, characteristics such as EA, hysteresis or SDC strongly depend on the maximum deformation in the cycle. A buffer deformed to 50% cannot return to 20% deformation due to plastic deformation. It will exhibit mechanical characteristics inherent to a deformation of 50%. A solution may be to place a mechanical limiter that would not allow deformation greater than a certain preset value.

Like all thermoplastics, TPE is characterised by low creep resistance. To reduce the negative effect of creep, a commercial filament made from a urethane thermoplastic elastomer can be used. These have numerous hydrogen bonds in the structure, which are stronger than the Van der Waals bonds found at the physical crosslinks of the network and have a creep-reducing effect in urethane TPEs [58].

CONCLUSIONS

For increasing values of material hardness (bumper type 1 vs. 2), number of model walls (bumper type 2 vs. 3) and infill density (bumper type 2 vs. 4 vs. 5) permanent set, energy absorption, hysteresis, specific damping capacity increase, but to different degrees.

The number of walls affects permanent set, energy absorption, hysteresis and specific damping capacity in a negligible way, i.e. a change in the number of walls from a minimum of 3 to a maximum of 8 does not have the same effect as, for example, a change in material hardness (from UNIFLEX 75 to UNIFLEX 120) or filling density (from 50% to 100%).

A given type of buffer can be characterised by its maximum load, plastic deformation and the

highest value of energy dissipated in the way of heat, i.e. hysteresis. For example, a bumper with a low hardness material can be characterised by a maximum permissible load of up to 0.635 kN, a plastic deformation of up to 11.0 % and a maximum hysteresis of 0.32 J. It can be used as a bumper under equipment with a low weight of 260 kg (4 units of type 1 bumpers) or to protect doors and gates against impacts. It should be noted at this point that it is not possible to give an answer about the superiority of one parameter over the other; it all depends on the application and intended use of the buffer.

Given the scarcity of literature sources describing the behaviour of TPE prints in uniaxial compression, directions for further research work should be given:

- Fabrication of the system presented in this publication and verification if the damping exhibited by the buffers can be shaped by stacking buffers with different mechanical characteristics.
- Creation of a mathematical model combining the mechanical characteristics inherent in the buffer and printing parameters, such as infill density, number of print walls, height of the printed layer, printing speed, printing temperature, among others, along with their interactions.
- Analysis of creep of buffers subjected to static compressive forces or the effect of strain rate on mechanical characteristics

REFERENCES

1. Tuleja, J., Kędzierska, K., Sowa, M., Galor, P. Evaluation of the possibility of increasing the energy absorption efficiency of fender devices using the example of cylindrical fenders with additional structural elements applied. Energies 2023; 16, 1–9. https://doi.org/10.3390/en16031165
2. Shen, MY., Wu, CC., Chiou, YC. Enhance energy absorption of hollow-cylinder rubber fender using V-notch ring grooves. Ocean Eng. 2022; 255: 1–15. https://doi.org/10.1016/j.oceaneng.2022.111442 (in Polish) Standard buffers. AXTONE, 2024. Available from: https://www.axtoneglobal.com/pl-pl/transportation/standard-buffers-freight-wagons (Accessed: 26.11.2024).
3. Cavallo F., Ceulemans J., Gasner B., Martinez M., Grilli M., Meniere Y., Mayoral J., Papanikolaou V., Radev B., Rudyk I., Rungger M., Terzić K., Van den Bulcke H. Innovation trends in additive manufacturing. Patents in 3D printing technologies. European Patent Office, Munich, Germany, 2023. Available from: https://link.epo.org/web/service-support/publications/en-additive-manufacturing-study-2023-full-study.pdf (Accessed on: 27.11.2024).
4. Achillas C., Aidonis D., Iakovou E., Thymianidis M., Tzetzis D., A methodological framework for the inclusion of modern additive manufacturing into the production portfolio of a focused factory. J. Manuf. Syst. 2015; 37: 328–339, https://doi.org/10.1016/j.jmsy.2014.07.014
5. Dhir A., Talwar S., Islam N., Alghafes R., Badghish S., Different strokes for different folks: Comparative analysis of 3D printing in large, medium and small firms, Technovation. 2023; 125. https://doi.org/10.1016/j.technovation.2023.102792
6. León-Calero M. Vales S., Marcos-Fernandez A., Rodriguez-Hernandez J. 3D Printing of thermoplastic elastomers: role of the chemical composition and printing parameters in the production of parts with controlled energy absorption and damping capacity. Polymers 2021; 13(20): 1–26. https://doi.org/10.3390/polym13203551
7. Rajamani P., Ageyeva T., Kovacs J. Personalized mass production by hybridization of additive manufacturing and injection molding. Polymers 2021; 13(2): 1–19, https://doi.org/10.3390/polym13020309.
8. Ligon, S., Liska, R., Stampfl, J., Gurr, M., Mulhaupt, R. Polymers for 3D printing and customized additive manufacturing. Chem. Rev. 2017; 117(15): 10212–10290, https://doi.org/10.1021/acs.chemrev.7b00074
9. Vithani K., Goyanes A., Jannin V., Basit A., Gaisford S., Boyd B. An Overview of 3D Printing Technologies for Soft Materials and Potential Opportunities for Lipid-based Drug Delivery Systems. Pharm. Res. 2019; 36(4): 1–20, https://doi.org/10.1007/s11095-018-2531-1
10. Zhou L., Fu J., He Y. A Review of 3D printing technologies for soft polymer materials. Adv. Funct. Mater. 2020; 30(28): 1–38. https://doi.org/ 10.1002/adfm.202000187
11. Elsonbaty A., MRashad A., Omnia A., Abdelghany T., MAlfauiomy A. A survey of fused deposition modeling (FDM) technology in 3D printing. J. Eng. Res. 2024; 26(11): 304–312. https://doi.org/10.9734/jerr/2024/v26i111332
12. Boschetto A., Bottini L., Veniali F., Finising of fused deposition modeling parts by CNC machining. Robot. Comput.-Integr. Manuf. 2016; 41: 92–101. https://doi.org/ 10.1016/j.rcim.2016.03.004
13. Singh R., Singh S., Singh I., Fabbrocino F., Fraternali F. Investigation for surface finish improvement of FDM parts by vapor smoothing process. Compos. B: Eng. 2017; 111: 228–234. https://doi.org/10.1016/j.compositesb.2016.11.062

14. Pazhamannil R., Namboodiri V., Govindan P., Edacherian A. Property enhancement approaches of fused filament fabrication technology: A review. Polym. Eng. Sci. 2022; 62(5): 1356–1376. https://doi.org/10.1002/pen.25948
15. Giubilini A., Minetola P. Multimaterial 3D printing of auxetic jounce bumpers for automotive suspensions. Rapid Prototyp. J. 2023; 29(11): 131–142. https://doi.org/10.1108/RPJ-02-2023-0066
16. Sola A. Materials requirements in fused filament fabrication: A framework for the design of next-generation 3D printable thermoplastics and composites. macromol. Mater. Eng. 2020; 307(10): 1–40. https://doi.org/10.1002/mame.202200197
17. Chung D. Materials for vibration damping. J. Mater. Sci. 2001; 36(24): 5733–5737. https://doi.org/10.1023/A:1012999616049
18. Puskas J., Antony P., El Fray M., Altstadt V. The effect of hard and soft segment composition and molecular architecture on the morphology and mechanical properties of polystyrene-polyisobutylene thermoplastic elastomeric block copolymers. Eur. Polym. J. 2003; 39: 2041–2049. https://doi.org/10.1016/S0014-3057(03)00130-7
19. Preiss D., Skinner D. Damping characteristics of elastomers. Rubber Age. 1965; 97(5): 58–68.
20. Puskas J., El Fray M., Tomkins M., Dos Santos L., Fischer F., Altstadt V. Dynamic stress relaxation of thermoplastic elastomeric biomaterials. Polymer. 2009; 50(1): 245–249. https://doi.org/10.1016/j.polymer.2008.10.030
21. Bergstrom J., Boyce M. Constitutive modeling of the large strain time-dependent behavior of elastomers. J. Mech. Phys. Solids. 1998; 46(5): 931–954. https://doi.org/10.1016/S0022-5096(97)00075-6
22. Szymczyk A., Nastalczyk J., Sablong R., Roslaniec Z. The influence of soft segment length on structure and properties of poly(trimethylene terephthalate)-block-poly(tetrametylene oxide) segmented random copolymers. Polym. Adv. Technol. 2011; 22: 72–83. https://doi.org/10.1002/pat.1858
23. Drobny J.G. Handbook of Thermoplastic Elastomers. Second Edition. Amsterdam, Netherlands: Elsevier Ltd.; 2014.
24. Mark J.E., Burak E., Frederick R.E. The science and technology of rubber. Third Edition. Amsterdam, Netherlands: Elsevier Ltd.; 2005.
25. Konyukhova E., Neverov V., Godovsky Y., Chvalun S., Soliman M. Deformation of polyether-polyester thermoelastoplastics: Mechanothermal and structural characterisation. Macromol. Mater. Eng. 2002; 287(4): 250–265. https://doi.org/10.1002/1439-2054(20020401)287:4<250::AID-MAME250>3.0.CO;2-Z
26. Prisacariu C. Polyurethane Elastomers. From morphology to mechanical aspects. First Edition. Wien, Austria: Springer-Verlag; 2011. Mechanical aspects of polyurethane elastomers. 103–202.
27. Persson A., Andreassen E. Cyclic compression testing of three elastomer types-a thermoplastic vulcanizate elastomer, a liquid silicone rubber and two ethylene-propylene-diene rubbers. Polymers. 2022; 14(7): 1–32. https://doi.org/10.3390/polym14071316
28. Versteegen R. Well-defined Thermoplastic Elastomers. Reversible networks based on hydrogen bonding [PhD dissertation on the Internet]. Eindhoven: Technische Universiteit Eindhoven; 2003. Available from: https://pure.tue.nl/ws/portalfiles/portal/1766324/200310704.pdf
29. Sharma S., Kar KK. Composite Materials. Processing, Applications, Characterizations. First edition. Berlin, Germany: Springer-Verlag; 2017. Newly Developed Rubber Pressure Molding Technique for Fabrication of Composites. 79–88.
30. Mahmood S., Talamona D., Goh K., Qureshi A. Fast Deviation Simulation for 'Fused Deposition Modeling' Process. Proceedings of the: 14th CIRP Conference on Computer Aided Tolerancing (CAT). 2016; Gothenburg, Sweden. Elsevier B.V. 327–332.
31. Kechagias J., Chaidas D., Vidakis N., Salonitis K., Vaxevanidis N. Key parameters controlling surface quality and dimensional accuracy: a critical review of FFF process. Mater. Manuf. Process. 2022; 37(9): 963–984. https://doi.org/10.1080/10426914.2022.2032144
32. Christ J., Aliheidari N., Potschke P., Ameli A. Bidirectional and stretchable piezoresistive sensors enabled by multimaterial 3D printing of carbon nanotubethermoplastic polyurethane nanocomposites. Polymers. 2019; 11(11): 1–16. https://doi.org/10.3390/polym11010011
33. Kim K., Park J., Suh J., Kim M., Yeong Y., Park I. 3D printing of multiaxial force sensors using carbon nanotube (CNT)/thermoplastic polyurethane (TPU) filaments. Sens. Actuators A: Phys. 2017; 263: 493–500. https://doi.org/10.1016/j.sna.2017.07.020
34. Hu GF., Damanpack AR., Bodaghi M., Liao WH. Increasing dimension of structures by 4D printing shape memory polymers via fused deposition modeling. Smart Mater. Struct. 2017; 26(12). https://doi.org/10.1088/1361-665X/aa95ec
35. Zhou F., Zhang M., Cao X., Zhang Z., Chen X., Xjao Y., Liang Y., Wong T., Li T., Xu Z. Fabrication and modeling of dielectric elastomer soft actuator with 3D printed thermoplastic frame. Sens. Actuators A: Phys. 2019; 292: 112–120. https://doi.org/10.1016/j.sna.2019.02.017
36. Calascione T., Fischer N., Lee T., Thatcher H., Nelson-Cheeseman B. Controlling magnetic properties of 3D-printed magnetic elastomer structures via

fused deposition modeling. In: Proceedings of the 65th Annual Conference on Magnetism and Magnetic Materials (MMM), Palm Beach, 2021. https://doi.org/10.1063/9.0000220

37. Rodriguez-Parada L., de la Rosa S., Mayuet P. Influence of 3D-Printed TPU Properties for the Design of Elastic Products. Polymers. 2021; 13(15): 1–21
38. Paz E., Jimenez M., Romero L., Del Mar Espinosa M., Dominguez M. Characterization of the resistance to abrasive chemical agents of test specimens of thermoplastic elastomeric polyurethane composite materials produced by additive manufacturing. J. Appl. Polym. Sci. 2021; 138(32): 1–11. https://doi.org/10.1002/app.50791
39. Haryńska A., Gubańska I., Kucińska-Lipka J, Janik H. Fabrication and characterization of flexible medical-grade TPU filament for FDM 3DP technology. Polymers. 2018; 10(1304). https://doi.org/10.20944/preprints201810.0552.v1
40. Jung S., Lee S., Kim H., Park H., Wang Z., Kim H., Yoo J., Chung S., Kim H. 3D printed polyurethane prosthesis for partial tracheal reconstruction: a pilot animal study. Biofabrication. 2016; 8(4). https://doi.org/10.1088/1758-5090/8/4/045015
41. De Leon A., Dominguez-Calvo A., Molina S. Materials with enhanced adhesive properties based on acrylonitrile-butadiene-styrene (ABS)/thermoplastic polyurethane (TPU) blends for fused filament fabrication (FFF). Mater. Des. 2019; 182: 1–11. https://doi.org/10.1016/j.matdes.2019.108044
42. Arifvianto B., Satiti BE., Salim UA., Suyitno S., Nuryanti A., Mahardika M. Mechanical properties of the FFF sandwich-structured parts made of PLA/TPU multi-material. Prog. Addit. Manuf. 2022; 7(6): 1213–1223. https://doi.org/10.1007/s40964-022-00295-6
43. Kumar N., Jain P., Tandon P., Pandey P. Additive manufacturing of flexible electrically conductive polymer composites via CNC-assisted fused layer modeling process. J. Braz. Soc. Mech. Sci. Eng. 2018; 40(175): 1–13. https://doi.org/10.1007/s40430-018-1116-6
44. Kumar N., Jain P., Tandon P., Pandey P. The effect of process parameters on tensile behavior of 3D printed flexible parts of ethylene vinyl acetate (EVA). J. Manuf. Process. 2018; 35: 317–326. https://doi.org/10.1016/j.jmapro.2018.08.013
45. Saari M., Galla M., Cox B., Krueger P., Cohen A., Richer E. Additive manufacturing of soft and composite parts from thermoplastic elastomers. 2015; 949–958.
46. Lathers S., Mousa M., La Belle J. Additive manufacturing fused filament fabrication three-dimensional printed pressure sensor for prosthetics with low elastic modulus and high filler ratio filament composites. 3D Print. Addit. Manuf. 2017; 4(1): 30–40. https://doi.org/10.1089/3dp.2016.005
47. Wojnowski J., Chmiel J. Personalized Anti-Vibration Protection for Telematics Devices in Urban Freight Transport Vehicles. Energies. 2021; 14(4193): 1–20. https://doi.org/10.3390/en14144193
48. Khan S., Joshi K., Deshmukh S. A comprehensive review on effect of printing parameters on mechanical properties of FDM printed parts. Proceedings of the 2nd International Conference on Functional Material, Manufacturing and Performances (ICFMMP). 2021; Phagwara, India. 2119–2127. https://doi.org/10.1016/j.matpr.2021.09.433
49. Xu P., Qu C., Yao S., Yang C., Wang A. Numerical Optimization for the Impact Performance of a Rubber Ring Buffer of a Train Coupler. Machines. 2021; 9(10): 1–20. https://doi.org/10.3390/machines9100225
50. Monkova K., Vasina M., Zaludek M., Monka P., Tkac J. Mechanical vibration damping and compression properties of a lattice structure. Materials. 2021; 14(6): 1–16. https://doi.org/10.3390/ma14061502
51. Kechagias J., Vidakis N., Petousis M. Parameter effects and process modeling of FFF-TPU mechanical response. Mater. Manuf. Process. 2021; 38(3): 341–351. https://doi.org/10.1080/10426914.2021.2001523
52. Bates S., Farrow I., Trask R. Compressive behaviour of 3D printed thermoplastic polyurethane honeycombs with graded densities. Mater. Des. 2019; 162: 130–142. https://doi.org/10.1016/j.matdes.2018.11.019
53. Kar K., Bhowmick A. Hysteresis loss in filled rubber vulcanizates and its relationship with heat generation. J. Appl. Polym. Sci. 1997; 64(8): 1541–1555. https://doi.org/10.1002/(SICI)1097-4628(19970523)64:8<1541::AID-APP12>3.0.CO;2-0
54. Buckley C., Prisacariu C., Martin C. Elasticity and inelasticity of thermoplastic polyurethane elastomers: Sensitivity to chemical and physical structure. Polymer. 2010; 51(14): 3213–3224. https://doi.org/10.1016/j.polymer.2010.04.069
55. Piesowicz E., Paszkiewicz S., Szymczyk A. Phase separation and elastic properties of poly(trimethylene terephtalate)-block-poly(ethylene oxide) copolymers. Polymers. 2016; 8(237): 1–14. https://doi.org/10.3390/polym8070237
56. Diani J., Fayolle B., Gilormini P. A review on the Mullins effect. Eur. Polym. J. 2009; 45(3): 601–612. https://doi.org/10.1016/j.eurpolymj.2008.11.017
57. Król P. Linear Polyurethanes. Synthesis Methods, Chemical Structures, Properties and Applications. First Edition. Leiden, Netherlands: VSP; 2008.